Metallurgical and Materials Engineering *Research paper*
Association of Metallurgical Engineers of Serbia AMES *https://doi.org/10.30544/764*

ASSESSMENT OF MECHANICAL AND TRIBOLOGICAL PERFORMANCE OF HYBRID Al/MoS_2/Al_2O_3 COMPOSITE BY GFRA

Hari Kiran Vuddagiri[1], Sivasankara Raju Rallabandi[2], Srinivas Vadapalli[3], Thimothy Pandi[4]*

[1]Department of Mechanical Engineering, Avanthi Institute of Engineering and Technology, Makavarapalem(V), Narsipatnam-531113, Andhra Pradesh, India
[2]Department of Mechanical Engineering, Aditya Institute of Technology and Management, Tekkali-532201, Andhra Pradesh, India
[3]Department of Mechanical Engineering, GITAM Institute of Technology, Visakhapatnam-530045, Andhra Pradesh, India
[4]Department of Mechanical Engineering, Lendi Institute of Engineering and Technology, Jonnada, Vizianagaram-535005, Andhra Pradesh, India

Received 24.11.2021
Accepted 07.03.2021

Abstract

This work emphasizes the mechanical and tribological performance of Al-Si/Al_2O_3/MoS_2 hybrid matrix composites. The composites are reinforced by varying weight percentages of Al_2O_3 (8%, 12%, and 16%) and MoS_2 (0%, 2%, and 4%), and were prepared by stir casting. As the weight percentage of Al2O3 grows in matrix, the composites performed better hardness and tensile strength. The addition of 2% wt. MoS_2 enhances the specific strength and tribological properties, according to the research. However, when compared to other composites studied, the Al/16% Al_2O_3 composite had improved mechanical properties. MoS_2 also aids the hybrid composite in achieving higher tribological characteristics while marginally lowering the specific strength. Taguchi orthogonal array (L_{27}) is used to design tribological performances with process parameters viz. applied load, sliding speed and weight % of Al_2O_3 as well the percentage of MoS_2 whereas wear rate (mm^3/m), wear (µm) and coefficient of friction were considered as the responses. A hybrid Grey–Fuzzy Reasoning Approach (GFRA) is used to optimize a multi-response for avoiding vagueness in decision making. The statistical analysis revealed that Al/2%MoS_2/16%Al_2O_3 composite has exhibited better wear resistance than other composites. The confirmation test is also conducted to validate the optimal condition obtained by ANOVA.

Keywords: AMCs; Al_2O_3; MoS_2; GRA; fuzzy; GFRA.

*Corresponding author: Hari Kiran Vuddagiri, *harikiran3285@gmail.com*

Introduction

Aluminium alloys are widely used in industrial relevance's owing to their inexpensive cost, high strength-to-weight ratio (in comparison to titanium), and corrosion resistance. Aircraft, vehicles, electric motors, and instrument components employ this alloy. Nevertheless, their low wear resistance is one of these alloys' main drawbacks. Al-Si base alloys are universally recommended due to very desirable features, such as good workability, good thermal conductivity, resistance to corrosion, and good bearing performance. The Al-Si alloy is commonly used in a lot of places where things get worn down, like brakes, pistons, cylinder liners, and motor casings. In wear-related applications, composites have emerged as strong competitors to overcome this vulnerability and meet the ever-growing demand for the latest technology [1–3].

Ceramic reinforcement outperforms all other types of reinforcement in terms of strength. A consequence of this is that they are frequently utilized as the principal reinforcement material in the creation of hybrid advanced composites. Although secondary reinforcement improves the material's performance, it does not degrade its initial quality. To achieve better mechanical and tribological properties, the optimal wt. percentage of reinforcement added to the composites. In addition, introducing a new attribute improves the performance of a hybrid composite. To reduce the weight of the composite, the primary feature must be achieved first, followed by superior physical, mechanical, and tribological characteristics [4, 5].

For the most part, when it comes to wear resistance, lubrication is critical to reducing wear and tear. When it comes to protecting wear components, it can be a challenge to develop a lubricant that extends over the interfaces of the wear components. Self-lubricating components include a lubricant that can be rapidly dispensed during the wear process. When it comes to solid lubricant parts, graphite (Gr) and molybdenum disulphide (MoS_2) are two of the most common ones[6–8].

Vinoth et al. [9] investigated the impact of mechanical and tribological behaviour of Al-Si10Mg/MoS_2 composites. They discovered that adding MoS_2 particles to composites decreases their hardness, elongation, and tensile strength. As compared to the base alloy, the wear rate of the composites with 2% MoS_2 and 4% MoS_2 is decreased by 55% and 65%, respectively. *Upadhyay and Kumar* [10] created ternary epoxy-graphene-MoS_2 composites and determined their properties such as thermo-mechanical, and tribological behaviour. They also experimented on binary composites (epoxy-graphene and epoxy- MoS_2) and found that when compared to ternary composites, MoS_2 decreased friction and wear rate. The ternary composite exhibited that 0.0023–0.0048 friction coefficient, and the wear rate reported around 1.22×10^{-7} – 1.44×10^{-7} mm^3/N-m. The inclusion of graphene in the polymer matrix minimizes the likelihood of negative reactions such as sulphide and oxides, resulting in reduced friction and wear.

Suresh and Sridhar [11] focus was on the preparation of aluminium hybrid composites AHCs with SiC and Gr particles, with up to 10% while investigating how to enhance hardness and dry sliding wear behaviour. The wear behaviour of AHCs was examined using CCD, which showed that Gr composites and base alloys outperform. In HMCs, due to Gr particles' combination, wear declines with relative velocity and rises with sliding distance and load. The wear strength of the composites has increased by adding 10% wt. B_4C and 5% wt. Gr. Composites have a much lower wear rate than the

base matrix. The main reason for controlling the wear of the composite is the formation of a mechanically mixed layer (MML) at the tribo-surface interface.

Pankaj et al. [12] studied the wear behaviour of A356 reinforced with B_4C (4 and 12%wt.) and Gr (4%wt.) composites. They used testing parameters such as load (1-3kg), sliding speed (100-300rpm) and at a constant sliding distance (4000m). They revealed that with the addition of B_4C and graphite to the A356 alloy, the wear loss of the composites was reduced. The high hardness of B_4C and the self-lubrication property of graphite particles, which act as a barrier to wear loss, may explain the increase in wear resistance. It can also be noted that increasing the amount of hard B_4C particles increases wear resistance; in the current study, increasing the wt. percentage of B_4C to 12 wt.% coupled with 4 wt.% of graphite particles increased wear resistance of the composite.

The statistical analysis to optimise the parameters of the conditional process influenced the response. Many of the optimisation techniques, such as Taguchi, Genetic Algorithm (GA), Artificial Bee Colony (ABC), Desirability Functional Analysis (DFA), Particular Swarm Optimization (PSO), Grey Relational Analysis (GRA), and Ant Colony Optimization (ACO), is a technique for optimising a procedure and determining the best performance and effectiveness to reduce the number of trial runs. Although many aluminium alloys' mechanical and wear properties are intensively investigated in dry environments, AHCs are given far less attention.

The optimisation of the process parameters involving multi-performance characteristics, such as the instance of surface roughness and energy consumption, has been integrated into a single performance characteristic with the combined Al-SiC attractiveness value, deliberate by *Ramanujam et al.* [13].

Hemanth et al. [14] investigated the tribological properties of an Al-Cu-Mg alloy using an extended Taguchi (L27) orthogonal array. On the multi-response data set that has been turned into a data set, signal-to-noise ratio analysis is used to establish the ideal condition. *Rajesh et al*. [15] used a GRA to investigate the multi-functionality of Al-SiC composites in terms of wear and friction loss reduction when with contact stress, % of SiC, sliding distance, or sliding speed were varying. To do this, *Rajak et al.* used vacuum-casting to produce marble-reinforced composites (1.5 - 6%) [16]. They used multi-criteria decision-making (MCDM) to examine the cumulative attributes of composites and reported that a composite with a wt.% of 4.5 was the best for bearing implementations. *Raju et al.* [17] investigated the tribological properties of Al-CSA composites by employing a Grey-Fuzzy approach. To optimise the multiple reactions, a hybrid grey-fuzzy concept was developed. They demonstrated that the Grey Fuzzy Reasoning (GFRA) methodology was compared to DFA, Grey Relational Analysis (GRG), and Fuzzy Logic to determine its reliability and accuracy.

It is self-evident that the addition of hard ceramic particles to aluminium alloy enhances the base metal/alloy. The majority of this study has focused on improving the mechanical properties of manufactured composites. Furthermore, research into the friction mechanism involving hybrid composites is still in its early stages. Some efforts use Gr as reinforcing filler to reduce friction; however, MoS_2, another promising solid lubricant, has yet to be researched. In addition, there is very little research on the wet tribology of hybrid composites in the literature. In other words, there is a great deal of room for further research when it comes to aluminium alloy MMC's tribological behaviour, as well as an extraordinary opportunity and limitless possibilities for the

researchers to enhance the tribological characteristics of aluminium composite materials by way of varying variables such as the size of reinforcement particles, the addition of various reinforcement hybrid composite types, and the change in the technique of manufacturing. The present study investigated the properties of Al-Si reinforced with Al_2O_3 and MoS_2. Particulate composites are prepared by stir casting technique which makes the proposed work innovative and novel. The authors strongly believe and make an effort to enhance properties like micro-hardness, tensile strength, microstructure, corrosion and erosion resistance, and wear resistance to decrease the coefficient of friction.

The present work aimed at the optimization of tribological parameters of the Al-cast composite i.e., Al-based (C0), Al/2MoS_2 (C1), Al/4MoS_2 (C2), Al/8Al_2O_3 (C3), Al/12Al_2O_3 (C4), Al/16Al_2O_3 (C5), Al/8Al_2O_3/2MoS_2 (C6), Al/12Al_2O_3/2MoS_2 (C7), Al/16Al_2O_3/2 MoS_2 (C8), Al /8Al_2O_3/4MoS_2 (C9), Al/12Al_2O_3/4MoS_2 (C10), and Al/16Al_2O_3/4MoS_2 (C11). The wear behaviour of AMCs and AHCs is studied using a pin-on-disk machine. Process factors include load, MoS_2 and Al_2O_3 and sliding speed, while the responses are the friction, wear and wear rate. To achieve the lowest possible wear rate, the best level of wear behaviour parameters is required. Grey relation analysis (GRA) was used to optimise the combination of multiple responses. Multivariable systems using fuzzy logic theory improve the GRA's performance even further by refining it further. The Grey-Fuzzy uses a Taguchi orthogonal array to enhance wear behavioural parameters. ANOVA is used to identify the most important influencing variables, which aids in the development of greater dependability.

Materials and methods

Matrix material

Alloys made of aluminium and silicon (Al-Si) aren't the same as the phase diagram because aluminium has no solid solubility in silicon. This means that there will be no beta testing because there is no real-world problem to solve. The features of Al-Si alloys include low density, great corrosion resistance, and excellent castability. The inability to heat treat alloys is a major disadvantage. As a result, Mg is added to the alloy to improve its technical qualities. Secondary phase material (Mg_2Si precipitate) adds to the alloy's high strength properties by making it more durable. Table 1 details the composition of the substance. The MoS_2 particles were provided by Intelligent Materials Private Limited in Punjab, India, and the Al_2O_3 particulates were purchased from Sajan overseas private limited in Ahmadabad, India. The Malvern particle analyser (Model: Micro-P) is capable of determining the accuracy size distribution of particulates.

Table 1. Chemical Composition of Al-Si matrix.

Element	Si	Fe	Cr	Cu	Mn	Zn	Mg	Remain
Content (%)	0.8	0.8	≤ 0.2	≤ 0.1	≤ 0.05	≤ 0.05	≤ 0.01	Al

Fabrication of composites using stir casting route

Table 1Stir casting is used in this work, in which reinforced particles (Al_2O_3, MoS_2) are mixed in the liquid state via mechanical stirring. The stirring process enhanced

particles distribution into a semi-solid matrix. Compared with low viscosity, the combination of reinforcement particles was better at high matrix viscosity. In a graphite crucible, aluminium alloy (Table 1) is melted in a bottom pouring furnace at temperatures much above its liquid temperature, i.e. 750 °C. In the casting furnace, the crucible holds the molten aluminium.

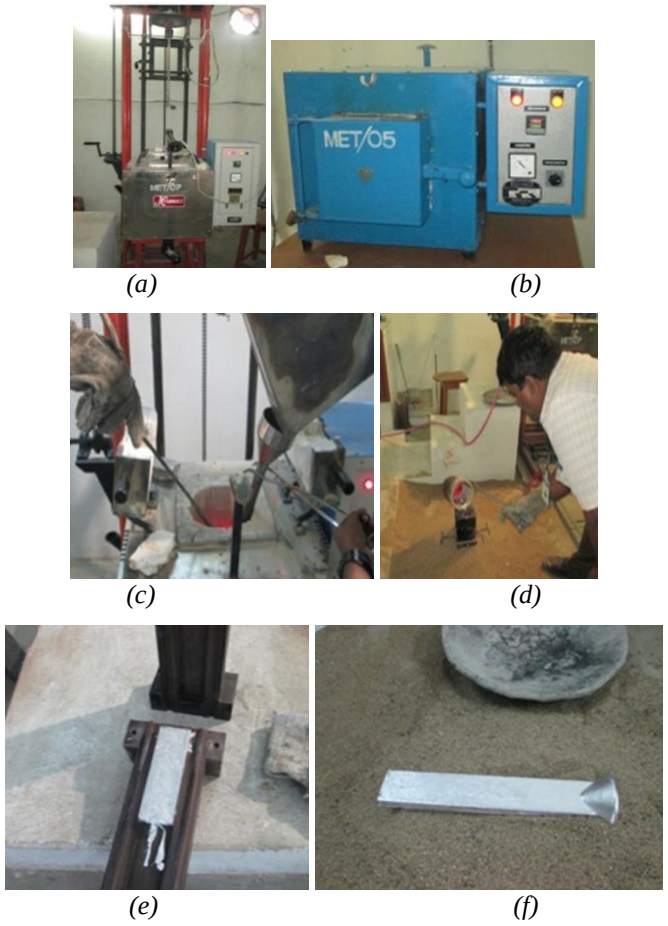

Fig. 1. Procedural sequence to make Al-composites: (a) bottom pouring furnace with stirrer set-up, (b) muffle furnace for preheating matrix and reinforcements, (c) pre-heated particulates poured into molten metal via chute, (d) pouring of molten metal into cast mould, (e) split of cast mould, (f) final product of cast composite.

The Al_2O_3 and MoS_2 particles were warmed for 2 hours at 500-600 °C to remove the accumulated synthetic hydroxyl layer and other surface gases. With a temperature just above 750 °C, the metal fully melted, the melt is left to cool between liquidus and solidus but is kept semi-solid. To improve wettability, magnesium ribbon (1 wt.%) was added to the metal mix before reinforcing. Three to four times the amount of reinforcement was poured into the molten and stimulated for ten minutes in the whirlpool. The mixture is

reprocessed to a liquid phase. The furnace is kept at 760 °C. As soon as the melt had been stirred, it was ladled into the casting mould to cool [18, 19]. Fig. 1 shows the sequence of casting operations, which were adapted for making the composite materials.

Testing methods of Al-composite materials

A variety of tests were performed under a variety of situations on Al-cast composites to establish their behaviour. The samples are established cast composites from the centre. Indentation values were taken into account using a hardness tester (Model RASN-B). The tensile test (Model: TUE-C-100) is used to measure the elasticity and strength of composites. The usual procedure is employed after the metallographic examination (ASTM E-7-17). To examine tribological qualities, a pin-on-disc tester (TE-165-LE, Magnum Engineers, Bangalore) with a sample size of ø 6mm and a length of 27 mm was utilised. Weight loss procedures are used to determine the wear rate (WR). The wear rate is measured in mm/m^2. Based on friction forces, the coefficient of friction has been computed [20,21]. The worn-out were examined SEM (Model: JEOL JSM-5600LV) and metallography samples using with Optical microscope (Model: METZ-797).

Experimental design

The Taguchi method is a robust design that defines a viable combination of design factors that minimises the cost of products and enhances quality with acceptable reliability. The experiments are intended to investigate the relationship between process parameters and responses such as wear (µm), wear rate (WR) and coefficient of friction (CF) for the cast composite have performed and listed in Table 2. Taguchi's L27 orthogonal array is used in this study, and the tests are performed on this cluster. The experimental design comprises four factors such as load, % of Al_2O_3, % of MoS_2 and sliding velocity are at three levels. Typically, the Taguchi method is used to optimise a single response; it is not effective at optimising multiple responses. As a result, it is important to transform multiple responses into a single comparable response to successfully implement the Taguchi approach and obtain the best possible parameter setting. Therefore, this study emphasizes GRA and GFRA based optimization for converting multi responses to a single response, for avoiding vagueness in decision making.

Table 2. Design of experiments with responses.

Run	Factors				Responses		
	Al_2O_3 wt.% (A)	MoS_2 wt.% (M)	Sliding Velocity (m/s) (V)	Load (N) (L)	Wear (µm)	WR (mm^3/m) ($\cdot 10^{-3}$)	CF
1	8	0	1	10	274	2.605	0.262
2	8	0	1.5	20	280	2.660	0.276
3	8	0	2	30	284	2.703	0.290
4	8	2	1	20	259	2.989	0.277
5	8	2	1.5	30	261	3.004	0.291
6	8	2	2	10	158	1.663	0.247
7	8	4	1	30	304	3.476	0.293
8	8	4	1.5	10	163	1.987	0.248

9	8	4	2	20	193	2.070	0.262
10	12	0	1	20	302	2.467	0.222
11	12	0	1.5	30	308	2.482	0.236
12	12	0	2	10	193	1.141	0.219
13	12	2	1	30	300	2.851	0.247
14	12	2	1.5	10	153	1.362	0.193
15	12	2	2	20	153	1.445	0.207
16	12	4	1	10	173	1.754	0.194
17	12	4	1.5	20	191	1.809	0.208
18	12	4	2	30	200	1.852	0.218
19	16	0	1	30	325	2.889	0.214
20	16	0	1.5	10	204	1.400	0.194
21	16	0	2	20	218	1.483	0.186
22	16	2	1	10	164	1.689	0.163
23	16	2	1.5	20	191	1.744	0.176
24	16	2	2	30	195	1.787	0.208
25	16	4	1	20	229	2.176	0.172
26	16	4	1.5	30	236	2.191	0.168
27	16	4	2	10	146	0.850	0.164

Grey Relational Analysis (GRA)

Normalization of tribological response values is done before the GRA study, so there is no difference in response units, strategic goals, or proportions. The results range between 0 and 1 by Equation (1) criteria, where the grey relational coefficient (GRC) is established by standardised data, more precisely through the alignment of the forecast and the actual Equation (2) empirical findings. The grey relational grade (GRG) for each response objective that the mean of the GRC indicates is then calculated using Equation (4). Generally, the GRG is built on many quality replies turned into a target sequence. The GRG simplified the general index of performance [22,23]. This shows that a higher GRG value implies better results.

$$X_i(k) = \frac{max\, y_i(k) - y_i(k)}{max\, y_i(k) - min\, y_i(k)} \qquad 1$$

The normalized grey relation value for the k^{th} argument is $X_i(k)$. The highest and lowest values of $y_i(k)$ for a k^{th} response values are max $y_i(k)$ and min $y_i(k)$. The number of variables (k=1 to 3) and the number of runs (i=1 to 27) are also important factors to consider.

$$\xi_i(k) = \frac{\Delta_{min} - \varsigma \Delta_{max}}{\Delta_{oi}\,(k) + \varsigma \Delta_{max}} \qquad 2$$

$$\Delta_{oi}\,(k) = \| x_o(k) - x_i(k) \| \qquad 3$$

$$\gamma_i = \frac{1}{n} \sum_{k=i}^{n} \xi_i(k) \qquad 4$$

Where Δ_{oi} (k) represents the difference of $x_0(k)$ and $x_i(k)$ with absolute meaning, in the reference series of variance.

Grey – Fuzzy Reasoning Analysis (GFRA)

Fig. 2Fuzzy logic deals with ambiguity and allows for the assimilation of different decision-making options, as well as providing an effective method for the construction of new strategies and approach variations with other techniques. Fuzzy logic is used to assess wear parameter optimisation in the multi-performance characteristic index (MPCI). The fuzzy is made up of three parts: a fuzzifier, an interface engine, and a defuzzifier. Fig. 2 depicts the fuzzy inference system's scheme, which includes three inputs and one output. Fuzzifier is a tool that converts inputs into a crisp format that includes information about unique linguistic factors. When using the fuzzifier integration function, the expert system uses fuzzy variables to represent erroneous requests. Triangular membership is evaluated in this study, as illustrated in Fig. 3. Fuzzy Set contains an enormous number of membership functions for unit intervals [0, 1]. Fig. 4 shows the linguistic variables that affect output. The knowledge base includes Mamdani and Sugeno. Although the rule foundation comprises logical IF-THEN rules operations, the package is fuzzy. Rule-based procedures are hampered by the interference mechanism. Using a defuzzifier allows you to get the precise information you need from a fuzzy system. It measures the GFRG output crisp or real values using the centre area methodology [24,25]. In comparison to GRA, the fuzzy logic solution provides altered GRG, which comprises a significant uncertain output. The degree of grey-fuzzy relation is above the degree of GRG. ANOVA explore the wear parameters from each input to lead to the optimum output. The intact approach incorporates both GRA and Fuzzy for optimal wear responses.

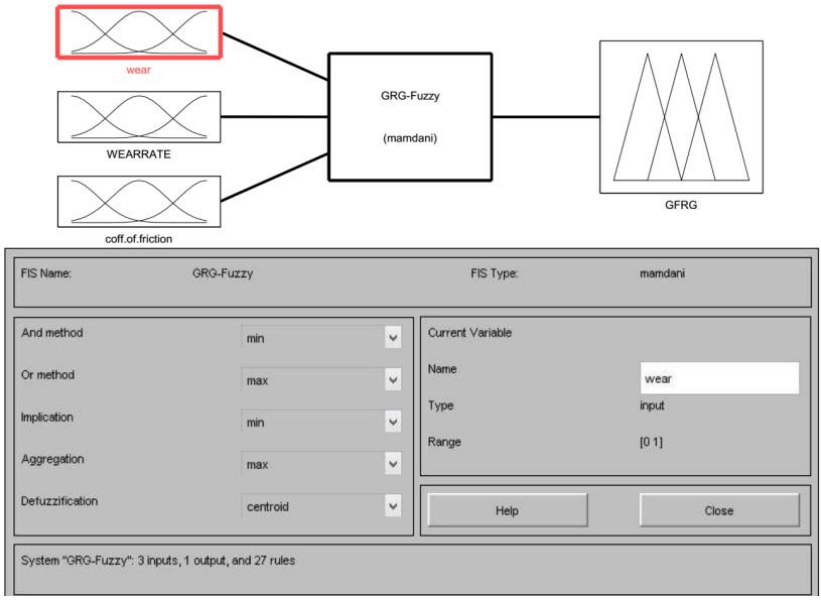

Fig. 2. Scheme of Fuzzy interface system.

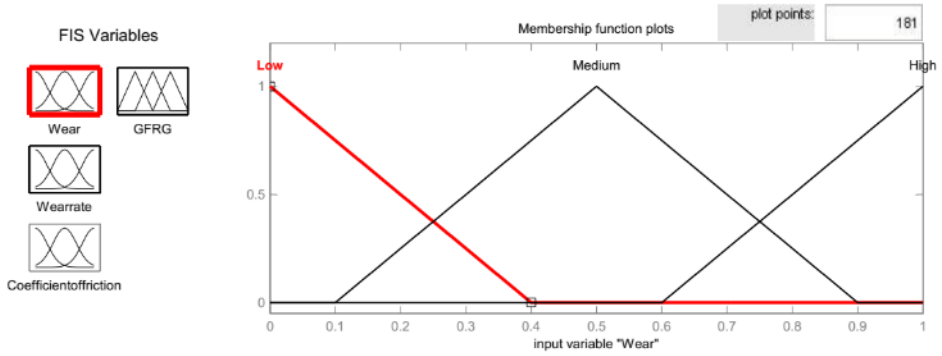

Fig. 3. Membership function for Fuzzy inference system input variables.

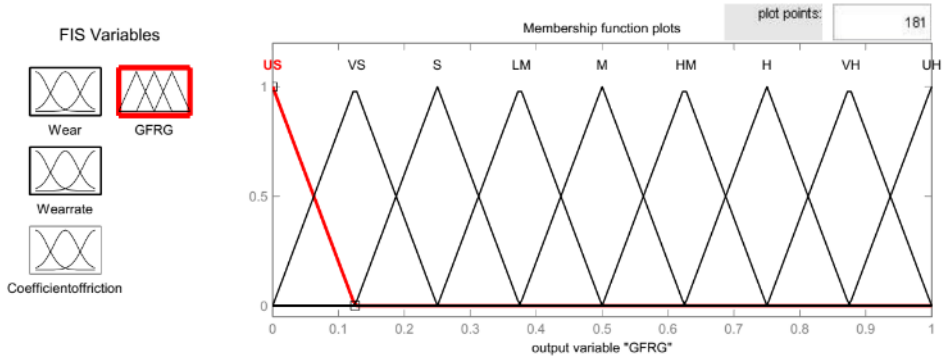

Fig. 4. Fuzzy Subset used for GFRG.

Results and discussion

A comparison of aluminium-composite patterns demonstrates that the peaks, as shown in Fig. 5, correlate to aluminium in the composites. Additionally, the peaks associated with molybdenum disulfide are observed in the aluminium composites C11. If Mg_2Si does occur as a result of the alloying materials being magnesium and silicon, it's not visible because of low temperatures during the process of sintering, which prevents the creation of Mg_2Si. Additionally, no peaks associated with other elements have been seen. The shape of reinforced particles (MoS_2 and Al_2O_3) is shown in Fig. 6 and Fig.7. The self-lubricated MoS_2 particles (vide in Fig. 6a), which are more spherical and flaky effectively penetrated the matrix. Fig. 6(b) displays the EDS spectrum, which exhibits peaks for Mo, S, O, and Al that originate from the substrate beneath the test sample. There are more elliptical or polyhedral-shaped Al_2O_3 particles (as shown in Fig. 7a). The size of the particles ranged from 10 to 60 microns, with a common particle size of 45 microns being used.

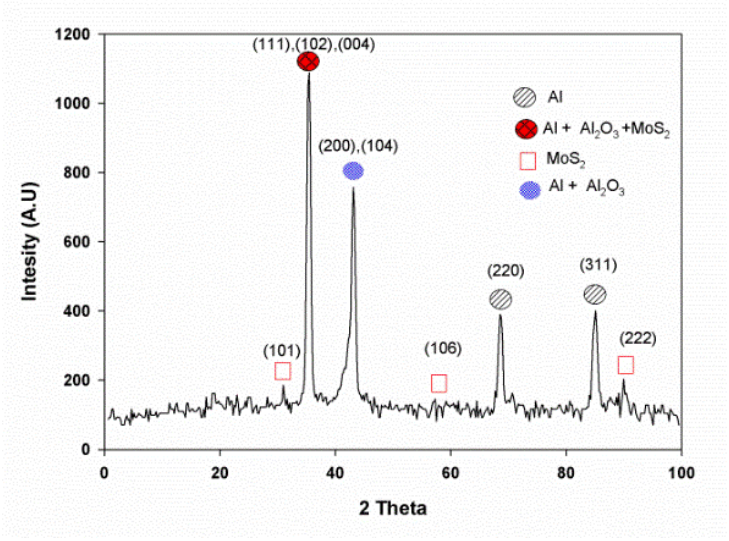

Fig. 5. X-ray diffraction of hybrid composite.

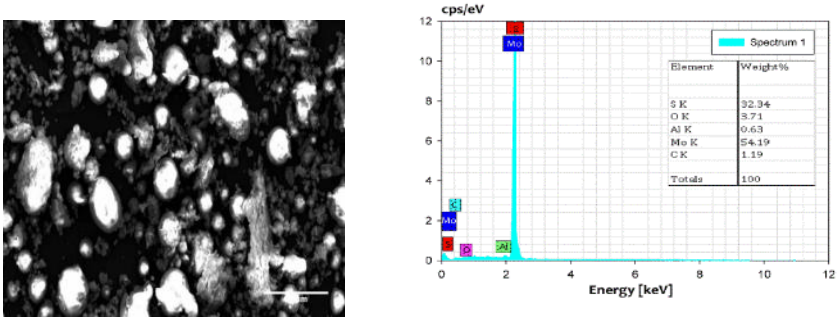

(a) *(b)*

Fig. 6. (a) SEM of Particles of MoS_2 (b) EDX of MoS_2 Particles.

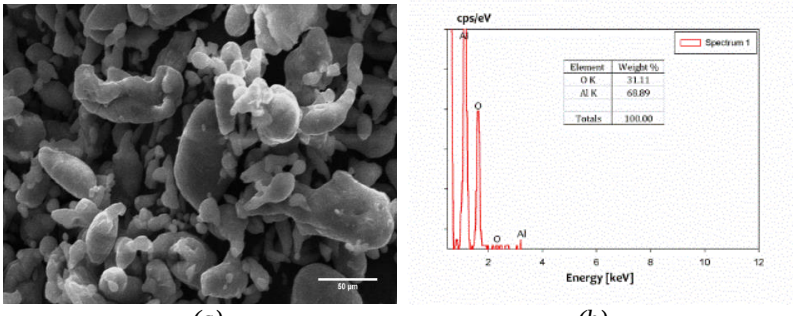

(a) *(b)*

Fig. 7. (a) Particles of Al_2O_3 (b) EDX of Al_2O_3 Particles.

Mechanical properties of composites

The ultimate tensile strength (UTS) of composites is shown in Fig. 8. The UTS of composites containing MoS_2 (i.e., C1, and C2) are decreased, thereby 6% and 11.75% as compared to the base matrix due to being softer in form. However, the composite C5 (Al/ 16% Al_2O_3) exhibited better UTS as compared to other composites. The hybrid composite i.e., C8 (Al-Si/ 2% MoS_2/ 16% Al_2O_3) strength increased by 5.07%, compared to C0. Similarly, the composite C11 exhibited better UTS than C9, C10, and C0. The composites exhibit a slight decrease in elongation compared to the base alloy, indicating that the addition of reinforcement (Al_2O_3 and MoS_2) reduced the composite's ductility, shown in Fig. 8. When compared to base alloy(C0), the elongation of MoS_2 composites (i.e., C1, and C2) is reduced by 18.67% and 24.70%, respectively. Furthermore, the C5 and C8 composites reduced elongation by 32.53% and 25.59%, respectively. Composites with this feature have an increased toughness. Hardness and elongation properties of composites are indirectly proportional characters, meaning if the hardness of the composite increases the elongation decreases.

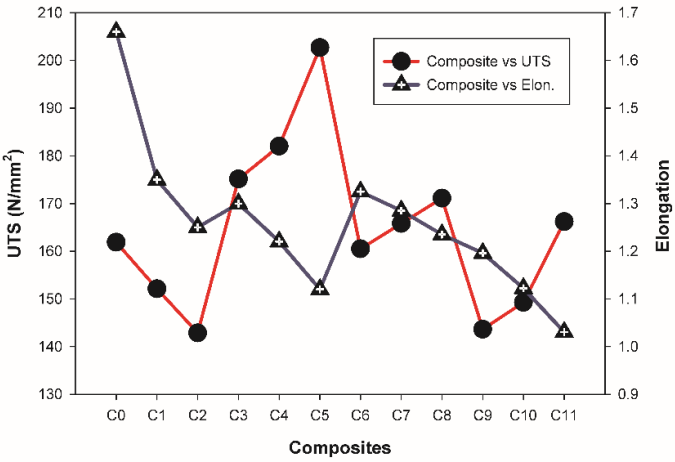

Fig. 8. Mechanical properties of composites (a) UTS (b) Elongation.

The hardness of composites (vide in Fig. 9) is enhanced with the increasing content of Al_2O_3 (C3, C4, and C5) and MoS_2 (C0, C1, and C2) reinforcement. The hard Al_2O_3particles in the hybrid composite, as well as their uniform distribution throughout the composite, are responsible for the increase in hardness. MoS_2 is a soft material with a lamellar structure. As a result, when compared to all other mono and hybrid composites, the mono-reinforced (i.e., 16% Al_2O_3; C5) composite exhibited higher hardness. As shown in Fig.9, increasing the Al_2O_3 concentration in the Al matrix will lead to an increase in the composite's density because the density of Al_2O_3 particulate is higher than the base alloy's (2.71 g/cm3). The density of MoS_2 (5.01 g/cm^3) is higher than that of aluminium alloy, hence increasing the weight proportion of reinforcement (Al_2O_3 and MoS_2) will raise the density of hybrid composites. There were 1.12% and 2.11% greater densities for mono composites C1 and C2 compared to the base alloys (C0). With increasing MoS_2 content in hybrid composites, the hardness and density of the composites

decreases. Similarly, Al_2O_3 composites density increased with Al_2O_3 weight percentage. The C8 hybrid composite increased 3.01% over the original matrix (C0).

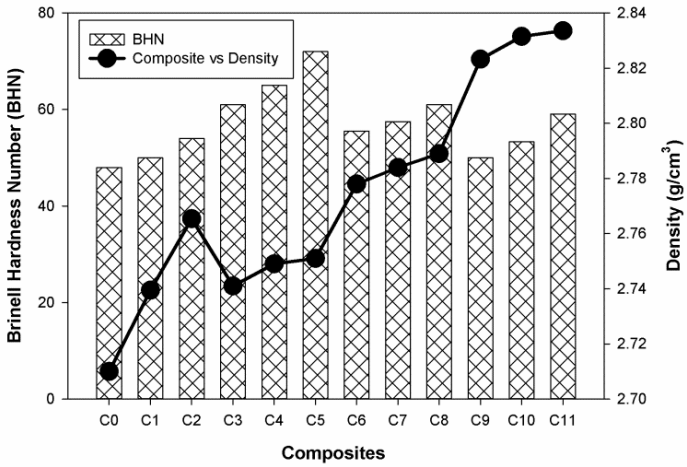

Fig. 9. Properties of composites: BHN, and density.

The volume percentage of alumina and the percentage of porosity contained in such hybrid composites were assessed using image analyser (Image-J) software. Density measurements were taken to ascertain the porosity of the composites created. This was accomplished through a comparison of the experimental and analytical densities for every wt.% composite. It is obvious that when the volume percentage of MoS_2 increases, the porosity level rises, affecting the composites harness. In the microstructural study, the porosity is readily visible. Similarly, as shown in (Fig. 10), the specific strength of the C10 (Al-Si /8%Al_2O_3 /4%MoS_2) composite was the lowest, which refers value is 52.40 N-m/kg, while C6 (Al-Si/16 % Al_2O_3) composite was the highest (75.89 N-m/kg).

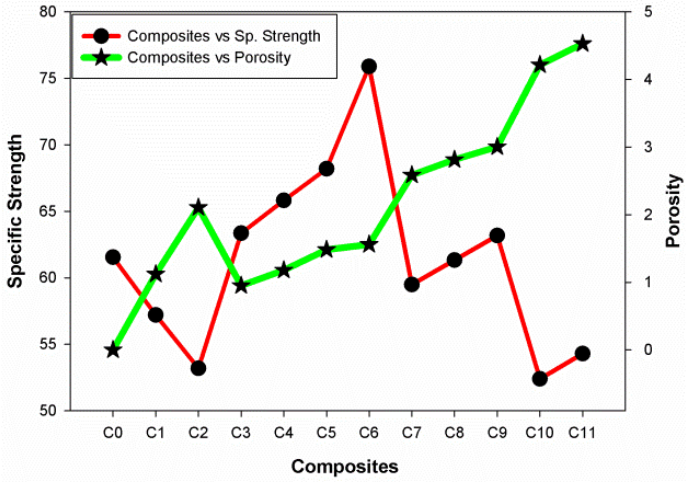

Fig. 10. Specific strength and porosity of composites.

Microstructural studies

The Optical micrographs of base alloy and composites ones (Fig. 11) indicated structure is dendritic in nature.

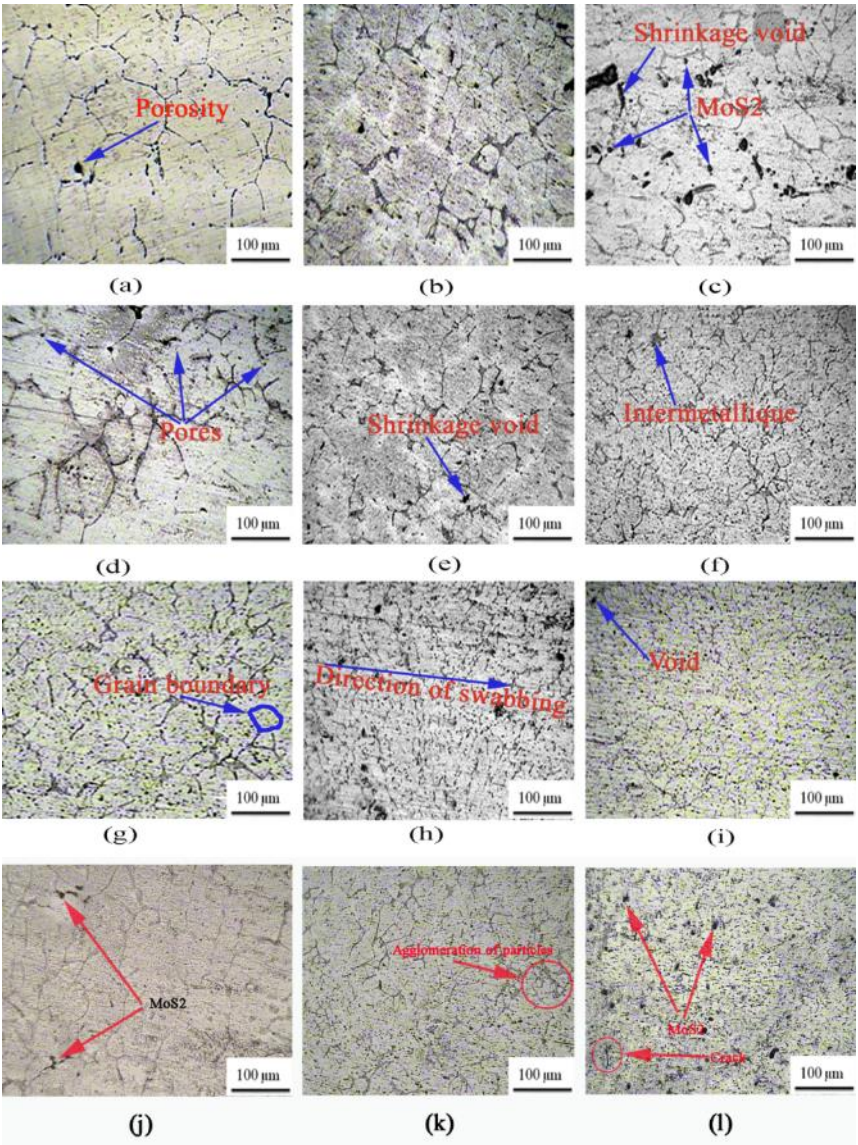

Fig. 11. Microstructure of composites (a)Al-base (C0), (b) Al/$_2$MoS$_2$ (C1), (c) Al/4MoS$_2$ (C2), (d) Al/8Al$_2$O$_3$ (C3), (e) Al/12Al$_2$O$_3$(C4), (f) Al/16Al$_2$O$_3$(C5), (g) Al/8Al$_2$O$_3$/2MoS$_2$ (C6), (h) Al/12Al$_2$O$_3$/2MoS$_2$ (C7), (i) Al/16Al2O$_3$/2 MoS$_2$ (C8), (j) Al /8Al2O3/4MoS$_2$ (C9), (k) Al/12Al2O$_3$/4MoS$_2$ (C10), and (l) Al/16Al2O$_3$/4MoS$_2$ (C11).

The composite C4 and C5 microstructures indicate that the grain structure is becoming progressively fine due to heterogeneous nucleation produced by the incorporation of Al_2O_3. When magnesium is added to the melt, it makes it more resistant to weight and makes particles more evenly distributed. Other characteristics of the microstructure involve relatively low porosity in the casting, an essential aspect of the composites produced. Aluminium dendrites solidify once the solid-liquid interface rejects them, and then they are divided into the interdendritic region [26]. Optical micrographs show the microstructures of Al alloy (C0) (Fig. 11a), Al/8Al_2O_3/2MoS_2 (Fig. 11g), Al/12Al_2O_3/2MoS_2 (Fig. 11h) and Al-Si/16Al_2O_3/2MoS_2 (Fig. 11i) hybrid composites. The grain content for the cast composite is generally much thinner compared to Al-alloy owing to chilling casting and augmented heterogeneous nucleation due to incoherent particles. As cast composites with fine grains have increased hardness and tensile strength. This structural refinement can be attributed to the heterogeneous nucleation caused by the MoS_2. Al/4MoS_2 composite displays the finest microstructure because of a higher fraction of MoS_2 addition. Optical micrographs show the microstructures of Al/12Al_2O_3/4MoS_2 (Fig. 11j), Al/12 Al_2O_3/4MoS_2 (Fig. 11k) and Al/4MoS_2/16Al_2O_3 (Fig. 11(l)) of hybrid composites have three distinct phases namely the Al_2O_3, Al and MoS_2 in a dendritic matrix. It is clear that a strong bond between matrix and reinforcement influences the wear mechanism of composites that decreases the rate of wear.

ANOVA of GRA

Tribological responses were determined and normalized through the GRA method through the corresponding equations. Therefore, the deviational sequence is calculated and illustrated in Table 3. Every wear behaviour response of GRC and GRG with rank, has been indexed in Table 4.

Table 3. Experimental results and GRA of Deviational Sequences.

Trails	Wear	WR	CF
Δ1	0.715	0.668	0.763
Δ2	0.748	0.689	0.869
Δ3	0.772	0.705	0.974
Δ4	0.633	0.616	0.880
Δ5	0.643	0.621	0.986
Δ6	0.067	0.111	0.644
Δ7	0.882	0.776	0.998
Δ8	0.093	0.209	0.655
Δ9	0.262	0.241	0.761
Δ10	0.870	0.815	0.455
Δ11	0.905	0.820	0.560
Δ12	0.262	0.310	0.432
Δ13	0.860	0.762	0.649
Δ14	0.037	0.195	0.229
Δ15	0.036	0.227	0.335
Δ16	0.150	0.319	0.241
Δ17	0.250	0.340	0.347
Δ18	0.304	0.357	0.423
Δ19	1.002	1.000	0.392

Δ20	0.321	0.433	0.238
Δ21	0.402	0.465	0.177
Δ22	0.102	0.344	0.000
Δ23	0.252	0.365	0.100
Δ24	0.273	0.381	0.346
Δ25	0.463	0.505	0.069
Δ26	0.501	0.511	0.038
Δ27	0.000	0.000	0.008

Table 4. Grey relation coefficient (GRC) for each response and grey relational grade (GRG) with ranks.

Trails	GRC			Grey relational Grade (GRG)	GRG RANK
	Wear	WR	CF		
ζ1	0.411	0.428	0.396	0.412	20
ζ2	0.401	0.420	0.365	0.395	25
ζ3	0.393	0.415	0.339	0.382	26
ζ4	0.441	0.448	0.362	0.417	19
ζ5	0.438	0.446	0.337	0.407	22
ζ6	0.882	0.819	0.437	0.713	5
ζ7	0.362	0.392	0.334	0.362	27
ζ8	0.843	0.705	0.433	0.660	8
ζ9	0.656	0.675	0.397	0.576	17
ζ10	0.365	0.380	0.524	0.423	18
ζ11	0.356	0.379	0.472	0.402	23
ζ12	0.656	0.618	0.537	0.603	14
ζ13	0.368	0.396	0.435	0.400	24
ζ14	0.931	0.719	0.685	0.779	3
ζ15	0.932	0.688	0.599	0.740	4
ζ16	0.769	0.610	0.675	0.685	7
ζ17	0.667	0.595	0.591	0.617	11
ζ18	0.622	0.584	0.542	0.582	16
ζ19	0.333	0.333	0.560	0.409	21
ζ20	0.609	0.536	0.677	0.607	12
ζ21	0.555	0.518	0.739	0.604	13
ζ22	0.831	0.592	1.000	0.808	2
ζ23	0.665	0.578	0.833	0.692	6
ζ24	0.647	0.567	0.591	0.602	15
ζ25	0.519	0.498	0.878	0.632	10
ζ26	0.499	0.495	0.929	0.641	9
ζ27	1.000	1.000	0.955	0.961	1

The dominant parameter is determined by ANOVA (Table 5), whereby the load is accompanied by the percentage of Al_2O_3 and the percentage of MoS_2. The average contribution of the variables is 98.23% of the total variance in GRA. The main effect plot (Fig. 12) for GRG which represents the optimal parameter condition for GRG has been

found as $A_3M_3V_3L_1$, which refers to the load (L) is the most influencing factor at level-1 (10N) followed by % of Al_2O_3 (A) at level 3 (16%) and % of MoS_2 (M) at level 3(4%) as well sliding velocity (V) at level 3 (2 m/s), refers the highest average grey relational grade.

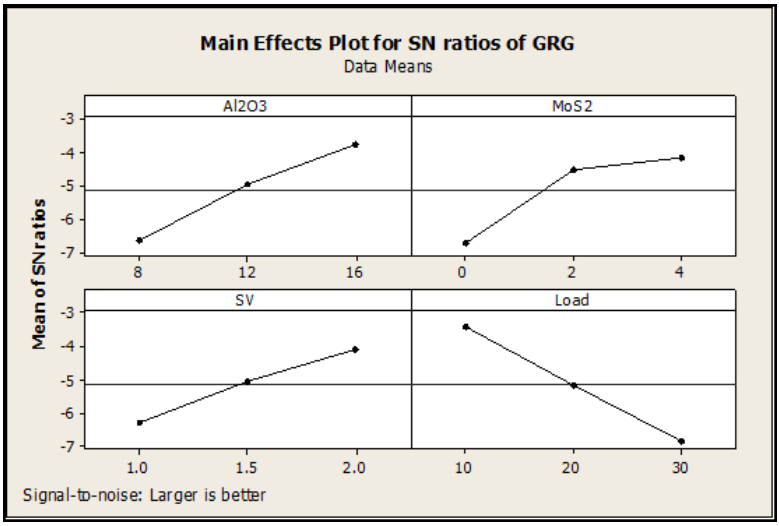

Fig. 12. Response graph for GRG value.

Table 5. ANOVA of GRG.

Source	DF	Seq SS	Adj MS	F	P
A	2	36.57	18.29	41.36	0
M	2	34.06	17.03	38.52	0
V	2	21.35	10.67	24.14	0.001
L	2	53.27	26.63	60.25	0
A*M	4	0.25	0.06	0.14	0.96
A*V	4	1.22	0.31	0.69	0.624
A*L	4	0.53	0.13	0.3	0.87
Error	6	2.65	0.44		
Total	26	149.90			

ANOVA for GFRG

Three normalized results are utilised as Fuzzy controller inputs. Assigning a triangular membership function to each response and then using a fuzzy rule to fuzzify the GRC are illustrated in Fig. 3. The input variable is employed in the form of three variations (Low (L), Medium (M) and High (H)) and the fuzzy subset (Fig. 4) is suited to GFRG. The input variables must be fuzzified with appropriate linguistic values. Following that, the centre of area method is used to estimate the crisp value (output) as a grey–fuzzy reasoning grade (GFRG). The nine linguistic variables are used as an output to generate 27 rules for calculating the GFRG using the MATLAB 7.0 software. In Table 6, the GFRG has confined data using the Center of Area (COA) method. Fig. 13 shows the GFRG value for a specific experiment (Expt. No. 14).

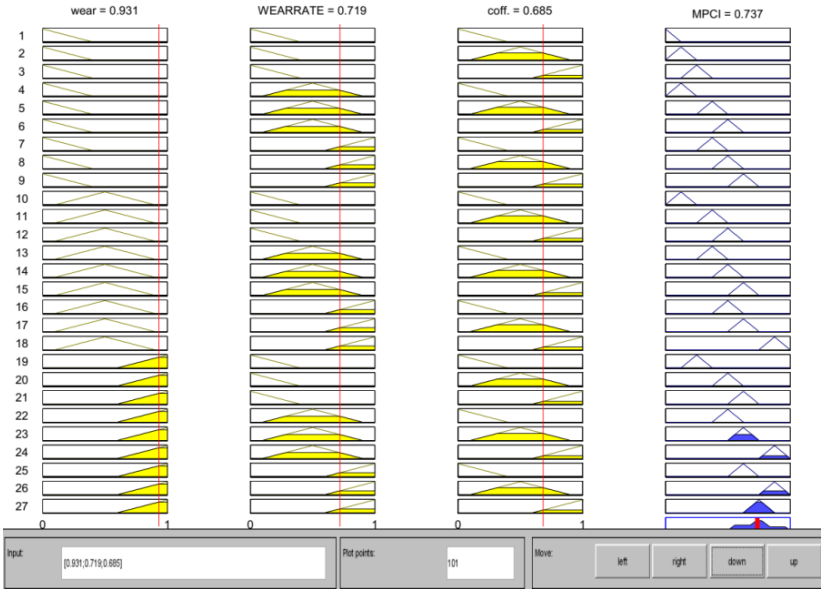

Fig. 13. The accumulation of centre of the area (COA) using crisp data for GFRA in run 14.

Table 6. Grey – Fuzzy grades and ranks.

Run	GFRG	Rank	Run	GFRG	Rank
1	0.508	18	15	0.751	5
2	0.494	19	16	0.648	12
3	0.470	23	17	0.569	17
4	0.492	20	18	0.612	15
5	0.481	21	19	0.467	24
6	0.799	3	20	0.658	11
7	0.425	27	21	0.670	10
8	0.705	9	22	0.967	2
9	0.614	14	23	0.792	4
10	0.461	25	24	0.625	13
11	0.456	26	25	0.737	8
12	0.574	16	26	0.750	6
13	0.478	22	27	0.976	1
14	0.737	7			

ANOVA (Table 7) shows the results of the GFRG. The highest impact parameter is load (44.29 %), followed by MoS_2 (12.22 %) and sliding speed (10.06 %). The combined contribution of GFRG for all factors involved is 94.78%. From the main effect plot (Fig. 14), it can be observed that the GFRG are high at the level of A_3(%of Al_2O_3 - 16%), M_2(%of MoS_2 -2%), V_3 (Sliding velocity-2 m/s) and L_1 (load-10N). the optimal value is $A_3M_2V_3L_1$.

Table 7. ANOVA of GFRG.

Source	DF	Seq SS	Adj MS	F	P
A	2	30.35	15.17	19.00	0.003
M	2	23.95	11.98	15.00	0.005
V	2	10.73	5.36	6.72	0.029
L	2	34.08	17.04	21.34	0.002
A*M	4	2.16	0.54	0.68	0.632
A*V	4	2.24	0.56	0.70	0.62
A*L	4	1.27	0.32	0.40	0.804
Error	6	4.79	0.80		
Total	26	109.57			

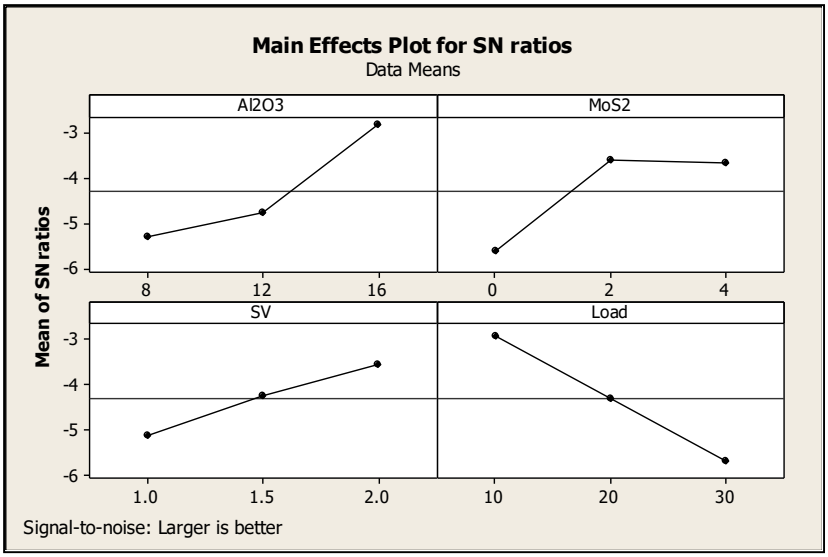

Fig. 14. Response graph for GFRG value.

Confirmation Test

Fig. 15 displays GRG and GFRG when contrasting to a maximum value at a statistical value near run 27. In the meantime, the GFRG grade change is easy, reducing confusion in decision making. The fuzziness is decreased and the grade importance of the reference value is closer to "1". Equation (5) calculates the expected grades (GRG and GFRG) at the optimum parameter stage.

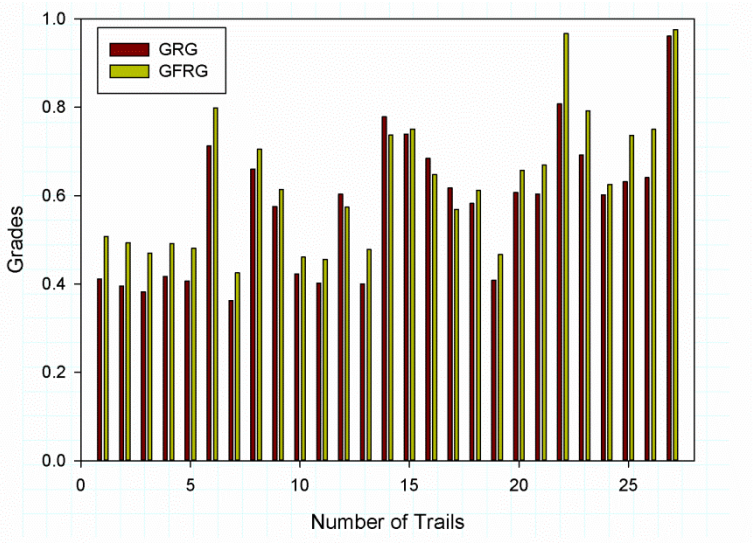

Fig. 15. Evaluation of grades for GRG and GFRG.

$$\eta_{predicted} = \eta_m + \sum_{i=1}^{k}(\bar{\eta}_i - \eta_m) \quad 5$$

Whereas (η_m) signifies the GRG of all the trials, and ($\bar{\eta}_i$) indicates the best assessment.

Table 8. Comparison of test combination with initial and optimal parameters.

Performance characteristics	A1M1V1L1	A3M2V3L1	A3M3V3L1	Gain	Improvement (%)	Error
GFRG experimental	0.523	0.782		0.259	33.12	-0.590
GFRG predicted	0.639	0.308		-0.331	107.47	
Wear	274	133		-141	106.22%	
Wear Rate	2.605	1.074		-1.531	142.50%	
Coefficient of friction	0.262	0.196		-0.066	33.91%	
GRG experimental	0.448		0.928	0.480	51.72	-0.960
GRG Predicted	0.73		0.250	-0.480	192.00	
Wear	274		102	-274	168.26%	
Wear Rate	2.605		0.688	-2.605	278.54%	
Coefficient of friction	0.262		0.151	-0.262	73.18%	

Table 2 shows the first conditional parameters (L1R1D1V1) from experiment number one. It is indicated in Table 8 that the initial GFRG value is 0.523 and the optimal GFRG value is 0.782 based on the confirmation test findings. As a result, utilising the grey-fuzzy reasoning technique (GFRA), GFRG in wear behavioural parameters of hybrid composites improved (33.12%) and the error is less than 5, which is significant. Table 9 shows that wear has been reduced from 133 µm to 102 µm, the coefficient of friction has been reduced from 0.196 to 0.151, and the wear rate has been lowered from 1.074 to 0.844 (mm^3/m). The initial parameters of the GRG and GFRG are 0.730, and 0.639, respectively, while the optimum conditional values of the GRG and GFRG are 0.851, and 0.928.

Table 9. The optimal condition for GRG and GFRG.

Responses	Optimal Condition		Gain by GFRG	Improvement (%)
	GFRG (A3M2V3L1)	GRG (A3M3V3L1)		
Wear	102	133	-31	30.09%
WR	0.688	1.074	-0.386	56.10%
CF	0.151	0.196	0.044	29.33%

Worn-out surface examination using SEM

Tests are carried out on the pin-on-disc device with a load of 30N, a sliding distance of 900 m, and an average sliding velocity of 1.5m/s, as shown in Fig. 16, to get SEM pictures of the substrate surface of Al-Si alloy and the cast composites, respectively. Abrasion and adhesion are the two main ways that the worn surface of the base alloy is changed. The marks 'X' and 'Y' show that (Fig. 16). There were deep sparkles, big drains on the worn surface, considerable burrs on the edge and plastic deformation resulting in an accelerated wear rate from abrasion (Mark 'X' in Fig. 16a). Abrasion (Mark 'Y' in Fig. 16a) is the fourth mechanism, which results from the high pressures between tribo-surfaces. Fig. 16(b) illustrates the used surface characteristics of the Al-Si /2%MoS_2 composite. Some of the surfaces have been worn away, and there are micro-cuts, very small waste, and burrs on the edges. When two pairs of moving parts are in contact with each other, they create an adhesive coating between them that decreases the deformations of their respective pin tracks. When examining the worn surface, it is possible to see a crisp delaminated layer that liberates the contacting pair and slows the rate of wear [10, 27, 28]. This is because oxide particles from Al_2O_3 have been plugged and broken up, so the tribo-surface of the Al-alloy /4Al_2O_3 substances (Fig. 16c) are mostly worn off on the pin surface. This indicates that the material is loose and adrift near the contact surface. A combination of contact between pairs, low hardness, and the flexible nature of aluminium are among the primary reasons for severe plastic deformation. The surface in Fig. 16d is smoother than Al-Si/4Al_2O_3. Particles are pressed out of the matrix as the proportion of Al_2O_3 increases, and mating lies on the disc as a result of this squeezing. The scattered particles also produced a load-bearing layer at the contact interface called the Mechanically Mixed Layer (MML). While friction is more prevalent and occurs more frequently at lower speeds, the layer cracks, leading to an increase in friction at higher speeds. As shown in Fig. 16e, there is a lot more severe plastic deformation in this hybrid composite than in other hybrid composites (Fig. 16f). The addition of Al_2O_3 refinement

and MoS_2 lubrication to a hybrid Al/2%MoS_2/12%Al_2O_3 composite modifies the worn surface of the alloy. The surface of the composite was found to be smooth, with a few small grooves and a lot of small particles. The burr near the border of the worn surface is quite minor as compared to the base matrix. When the load applied induces stresses exceeding fracture strength the Al_2O_3 and MoS_2 particles break and lose their efficiency as load-bearing components. The topographies of the surface used for the SEM images (Fig. 16g, and Fig. 16h) reveal the dominant wear mechanism. Depending on whether the Al_2O_3 particles are present, the degree of surface damage (i.e. the depth and width of the rains). Significant pull out of Al_2O_3 was observed. Fig. 16h shows a significant decline in the ploughing action of the shallow grooves indicated at 1.5 m/s, indicating a decline in the abrasive particle efficiency.

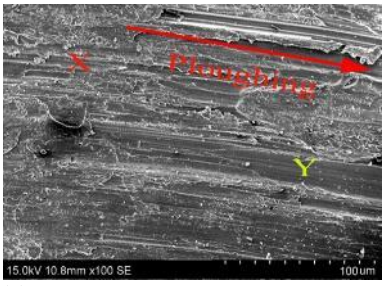

(a)

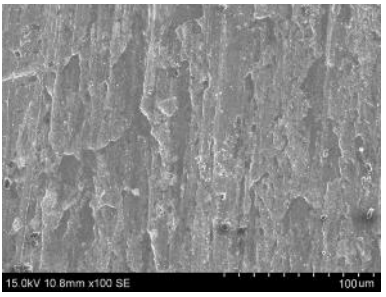

(b)

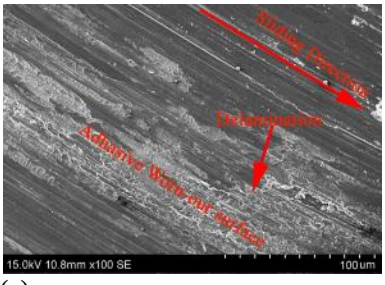

(c)

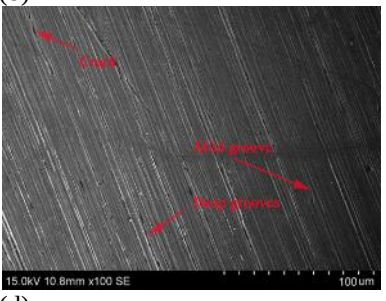

(d)

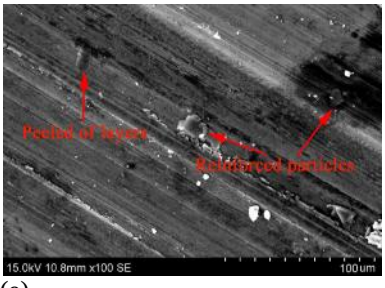

(e)

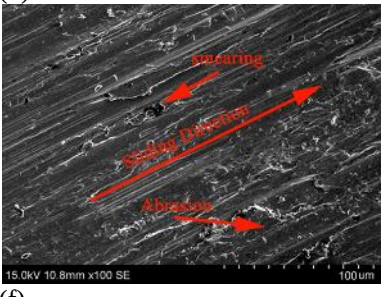

(f)

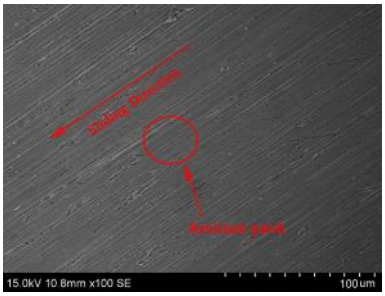

(g)

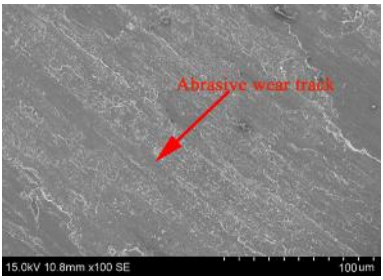

(h)

Fig. 16. (a) Al-Si (b) Al-Si/2MoS_2 (c) Al-Si /4Al_2O_3 (d) Al-Si/12 Al_2O_3 (e) Al-Si /2MoS_2 /8 Al_2O_3 (f) Al-Si /2MoS_2 /12Al_2O_3 (g) Al-Si /4MoS_2 /8Al_2O_3 (h) Al-Si /4MoS_2 /12Al_2O_3.

Similarly, an SEM photograph (Fig. 17) of a worn-out composite surface was tested under initial and optimal conditions, such as A1M1V1L1, A3M3V3L1, and A3M2V3L1. It reveals the formation of longitudinal grooves since the particles have been forced to remove and sheared out of the composite. This ensures here that the increased weight fraction of (Al_2O_3 and MoS_2) enhances the robust properties of the composites, in the way of the presence of MoS_2 film, working hard hindering the plastic deformation on the tribal surface and the composite achieved at a lower wear rate. SEM for the worn-out surface of the MoS_2 film has been found in many places with a rise in wear debris. It can be inferred that wear occurs at low speeds primarily due to ploughing and delamination.

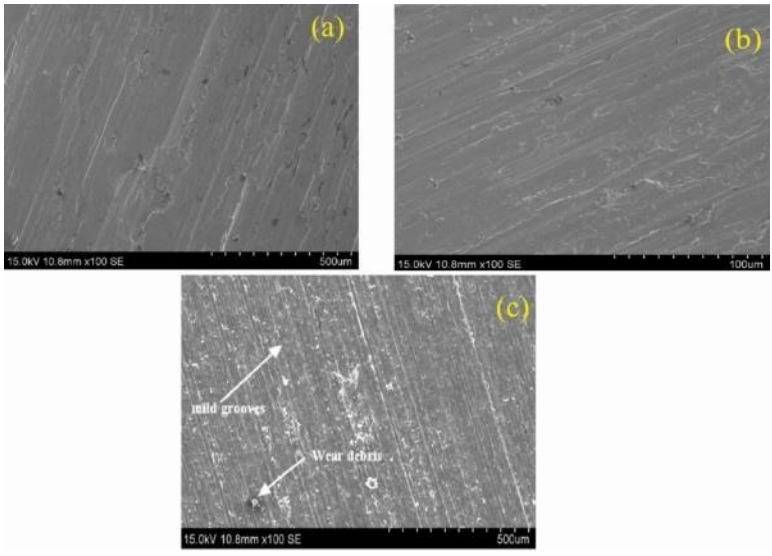

Fig. 17. Worn-out Surfaces at initial and optimal conditions (a) A1M1V1L1 (b) A3M3V3L1 (c) A3M2V3L1.

Conclusions

In this work, Al/MoS_2/Al_2O_3 composites are prepared with varying volume fractions of Al_2O_3 (i.e. 8%, 12%, and 16%) and MoS_2 (2% and 4%) via a stir casting process.

- Particles of Al_2O_3 have a more elliptical or polyhedral shape than those of MoS_2, which are more spherical and flaky in nature.
- The mechanical properties of composites are enhanced with increasing volume fraction of Al_2O_3, but elongation deteriorates.
- Taguchi OA (L27) is used to design the experiments with process parameters such as the percentage of Al_2O_3, the percentage of MoS_2, sliding velocity, and load whereas the responses are wear, wear rate, and coefficient of friction.
- Multi response optimization such as GRA and hybrid (grey-fuzzy) has been performed to obtain a single response and avoid ambiguity in decision-making.
- To optimize the tribological performance of the Al/MoS_2/Al_2O_3 composite, the input factors relating to the multi-performance characteristic index (GFRG) were analyzed to gain a better tribological response.
- Through the mathematical evolution of GRG and GFRG, it is observed that experiment number 27 is the best performance condition, which is closer to '1'.
- The analysis revealed, the effort parameters A3M3V3L1, and A3M2V3L1 produced the optimal condition for GRG and GFRG respectively.
- The results of validation show a decrease in wear from 133μm to 102μm, an improvement in friction coefficient from 0.196 to 0.151, and a reduction in wear rates from 1.074 to 0.844 (mm^3/m) respectively. The initial variable of the value of GRG, and GFRG is 0.730 and 0.639 by optimum conditional effects of GRG, and GFRG are 0.851 and 0.928.
- The overall improvement in GFRG as compared to GRG is 30.09%, 56.10%, and 29.33% in reducing wear, wear rate, and coefficient of friction to the initial condition.
- The worn-out surface examination is performed at optimal condition of GRG and GFRG, results of which corroborate with the findings.

Acknowledgements

The author would like to express his gratitude to Dr. Hota Ravisankar (Professor, Department of Mechanical Engineering, GITAM University, Vizag and Andhra Pradesh) for his generous support and role as a mentor throughout his professional career. However, on May 4, 2021, I heard of his untimely demise due to Covid-19. I'll keep in mind what you said to improve my career and decently help others. You are one of the institute's top teachers, researchers, and human beings. Your leadership, mentorship, and encouragement helped me grow as a person. It will stay with me for the rest of my life.

References

[1] C. Yan, W. Lifeng, R. Jianyue: Chinese J Aeronaut, 21 (2008) 578–584.
[2] Suraj Rawal: JOM, 53 (2001) 14–17.
[3] D. Manfredi, F. Calignano, M. Krishnan, R. Canali, E. Paola, S. Biamino, D. Ugues, M. Pavese, P. FinoAdditive Manufacturing of Al Alloys and Aluminium Matrix Composites (AMCs), in: Light Met. Alloy. Appl., InTech, 2014.
[4] P.D. Srivyas, M.S. Charoo: Metall Mater Eng, 27 (2021) 27–47.
[5] Alaneme K. k.; Adewuyi E.O.: Metall Mater Eng, 19 (2013) 177–187.
[6] R.S. Sankara Raju, M.K. Panigrahi, R.I. Ganguly, G. Srinivasa Rao: Tribol Int, 129 (2019) 55–66.
[7] M. Singh, B.K. Prasad, D.P. Mondal, A.K. Jha: Tribol Int, 34 (2001) 557–567.
[8] K.P. Furlan, J.D.B. de Mello, A.N. Klein: Tribol Int, 120 (2018) 280–298.
[9] K.S. Vinoth, R. Subramanian, S. Dharmalingam, B. Anandavel: Mater Tehnol, 46 (2012) 497–501.
[10] R.K. Upadhyay, A. Kumar: Tribiol Int, 130 (2019) 106–118.
[11] S. Suresha, B.K. Sridhara: Compos Sci Technol, 70 (2010) 1652–1659.
[12] P.R. Jadhav, M. Nagaral, S. Rachoti, J.I. Harti: J Met Mater Miner, 30 (2020) 106–112.
[13] R. Ramanujam, L.M. Maiyar, K. Venkatesan, M. Vasan: ARPN J Eng Appl Sci, 9 (2014) 457–463.
[14] T.R. Hemanth Kumar, R.P. Swamy, T.K. Chandrashekar: JMMCE, 10 (2011) 1179–1188.
[15] R. Siriyala, G. krishna Alluru, R. Penmetsa, M. Duraiselvam: Front Mech Eng, 7 (2012) 279–287.
[16] S.K. Rajak, A. Aherwar, D.R. Unune, M. Mia, C.I. Pruncu: Materials (Basel), 12 (2019) 1–16.
[17] S.R. Rallabandi, G. Srinivasa Rao: J Inst Eng Ser C, 100 (2019) 13–22.
[18] H.K. Vuddagiri, R.S. Hota: AIP Conf Proc, 020013 (2021) 1–11.
[19] R. S.S. Raju, V.S. B.: Int J Mater Eng Innov, 12 (2021) 83–102.
[20] Siva Sankara Raju, G. Srinivasa Rao, C. Samantra: Measurement, 140 (2019) 254–268.
[21] S.S. Raju, G.B. Murali, P.K. Patnaik: J Reinf Plast Compos, 39 (2020) 721–732.
[22] G. Rajyalakshmi, P. Venkata Ramaiah: Indian J Sci Technol, 8 (2015) 1–12.
[23] T. Rajmohan, K. Palanikumar: Measurement, 46 (2013) 1470–1481.
[24] R.S.S. Raju, G.S. Rao: Tribol Ind, 39 (2017) 364–377.
[25] R.K. Pandey, S.S. Panda: Meas J Int Meas Confed, 47 (2014) 386–392.
[26] J.F. Lin, C.C. Chou: Tribol Int, 35 (2002) 771–785.
[27] Y.C. Lin, J.N. Chen, Y.C. Huang, Y.H. Jian: Int J Surf Sci Eng, 9 (2015) 109–123.
[28] H.K. VUDDAGIRI, S. Vadapalli, J. Sagari, S.R. R.: Int J Automot Mech Eng, 18 (2021) 8959–8977.